COMITATO NAZIONALE PER L'ENERGIA NUCLEARE
Laboratori Nazionali di Frascati

LNF-72/16
18 Febbraio 1972

P. Spillantini : USE OF TOROIDAL MAGNETIC FIELD FOR EXPERIMENTATION WITH STORAGE RINGS. EVALUATION FOR ADONE. -

Servizio Documentazione
dei Laboratori Nazionali di Frascati del CNEN
Casella Postale 70 - Frascati (Roma)

Laboratori Nazionali di Frascati del CNEN
Servizio Documentazione

LNF-72/16
18 Febbraio 1972

P. Spillantini: USE OF TOROIDAL MAGNETIC FIELD FOR EXPERIMENTATION WITH STORAGE RINGS. EVALUATION FOR ADONE.

1. - INTRODUCTION. -

Almost all of the magnets proposed up to now for experimentation with storage rings can be put into two classes: magnets with the magnetic field perpendicular to the axis of the beam (z axis) (see Fig. 1a)[2, 3, 4, 7, 9, 10] and magnets with the magnetic field parallel to the axis of the beam (see Fig. 1b)[1, 5, 6, 7, 8, 11, 13] In particular for Adone a magnet of the first class (transversal solenoid and zero integral of the field at the axis of the beam) is already in an advanced stage of realization (now noted with the name MEA), and a magnet of the second class (non compensated longitudinal solenoid) has been recently proposed a bit in detail (with the conventional name MAL).

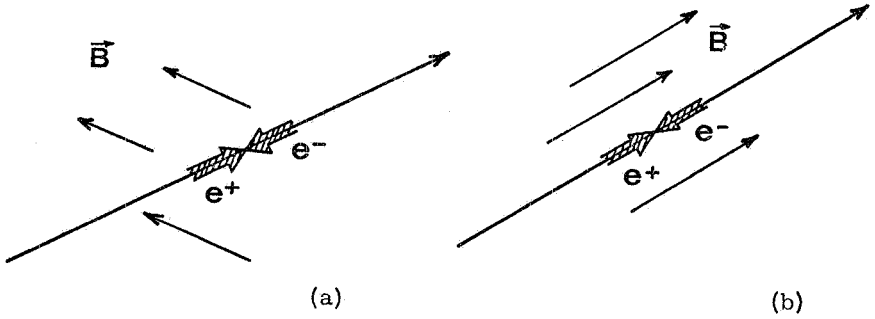

FIG. 1 - Transversal (a) and longitudinal (b) magnetic field.

For magnets of the first class it is necessary to cancel the magnetic field (or at least its integral) at the beam axis; the necessary compensators and the obstructions that they create right next to the beam pipe severely limit the solid angle accepted.

This compensation can be unnecessary for magnets of the second class if the value of the magnetic field is not too high; it is therefore possible to recover most of the solid angle. However, the fact that particles travel along paths curved in pla-

nes intersecting the axis of the beam destroys the most useful geometric aspect of reactions in storage rings, which is that the projection in a plane (x, y) perpendicular to the beam axis of the trajectories of all events becomes a certain number of straight lines emerging from a unique point well defined and easily reconstructed (see Fig. 2).

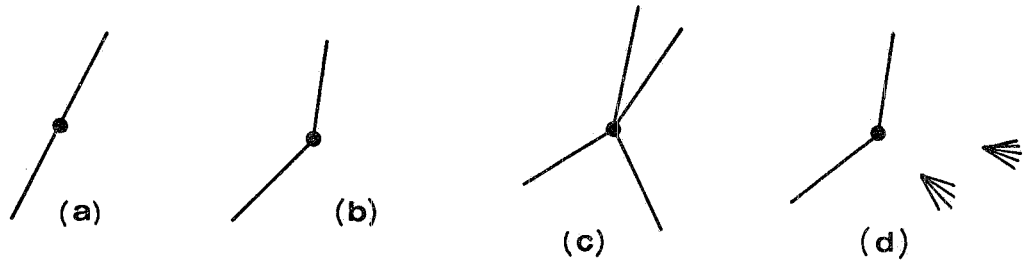

FIG. 2 - Geometrical configuration of projection in a plane perpendicular to the beam axis of some events in Adone. (a) - two complanar charged prongs; (b) two non complanar charged prongs; (c) four charged prongs; (d) two charged prongs and two converted γ rays.

This fact translates itself into a severe limitation to momentum band accepted since the realization of a trigger general enough and flexible enough becomes problematical.

Finally, the magnets of both classes have the magnetic field flux return completely external to the coil and require, therefore, a large mass of iron to contain it. The weight of this iron (and its cost) are much higher than that of the coil itself. In the case of Adone, for MEA and MAL, the weight of the iron are respectively 19 and 11 times that of the coil, and the price 8 and 5 times. Besides this large quantity of iron weighs heavily also on the dimension and price of the mechanical support, and these constitute an obstacle to the eventual external extension of the apparatus.

Probably this is the more significant inconvenience, because it prevents nearly completely the recognition of the nature of the particles by some external device, and indeed precludes a wide range of possible experiments.

The necessity of the external enclosure of the field flux imposes a limit also on the value of the field, since the volume of iron need to collect the return flux depends more than linearly on it. This amoung other things renders improbable or at least inconvenient the solution with magnets with superconducting coils, or, in any case, with magnets with a very high magnetic field.

Finally the encumbrance due to the iron needed to return the flux severely limits the solid angle utilizable for the detection of particles and the measurement of their momentum. This is very serious for the reactions with many final products for which it is very important to have a good probability to detect and possibly measure (possibly roughly) all of the particles produced, than to reconstruct the existence of lost particles from a precise measurement of momentum of those detected(x). For Adone in the most favorable case (the magnet MAL) this solid angle is 66% of the total, and the probability of missing one of the particles in an event with 4, 6 or 8 particles produced is very high, $\sim$ 81 %, 91 % and 96 % respectively (see Fig. 3).

(x) - In effect lossing a particle we loss information of two quantities (the θ and φ angles), while an improvement in momentum measurement improves the knowledge of only one quantity (the modulus of the momentum).

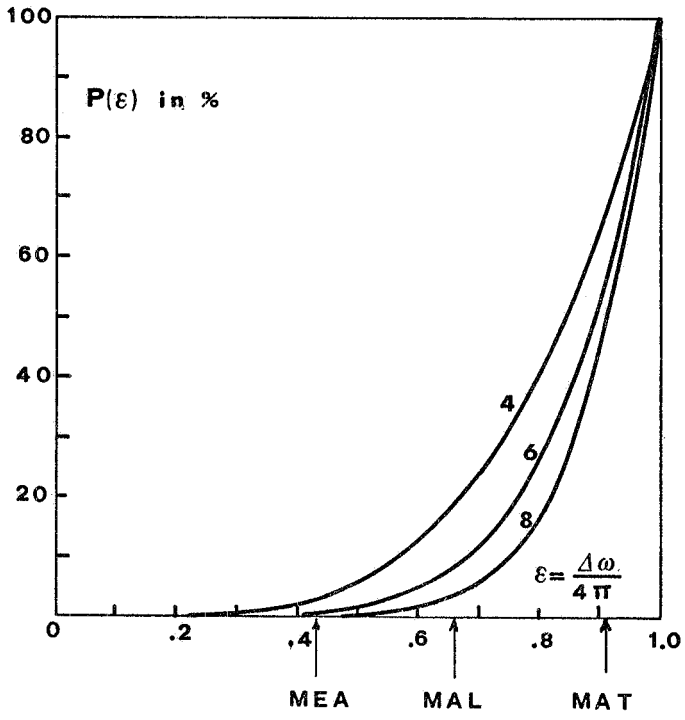

FIG. 3 - Probability P(ε) of not lossing any of produced particles in reactions with 4, 6 or 8 final particles, given as a function of fraction ε of accepted solid angle. (The particles are considered as independent).

2. - THE MAGNET WITH TOROIDAL FIELD (MAT). -

To overcome the difficulties explained above (the magnetic and mechanical linking with the beams, the loss of the simple geometry of the event, the return of the field flux, the limits to the maximum value of the field and to the solid angle accepted) a type of magnet with no external flux and with no field or derivative of the field at the axis of the beam is needed, giving up eventually the uniformity of the field inside the coils. Such a uniformity is of little importance provided that the dependence of the field on the spatial coordinates will be regular and not too strong.

A good solution is offered by a magnet of toroidal form as can be realized according to the following idea. A rectangular coil C with sides l and L lying in a plane π containing the beams with its side L parallel to it at a distance R_i (see Fig. 4); the direction of the magnetic field when the coil carries a current is normal to the plane π. If now we rotate the plane π about the axis of the beams, the coil describes a toroidal surface with the appearance indicated in Fig. 5. If one consider this sur-

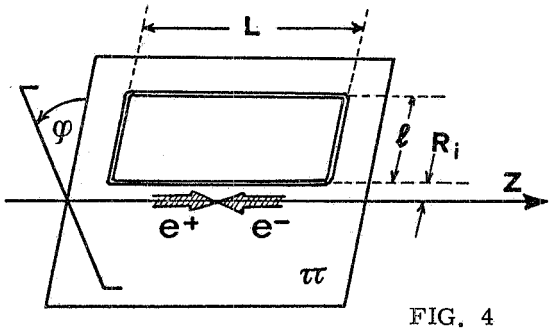

FIG. 4

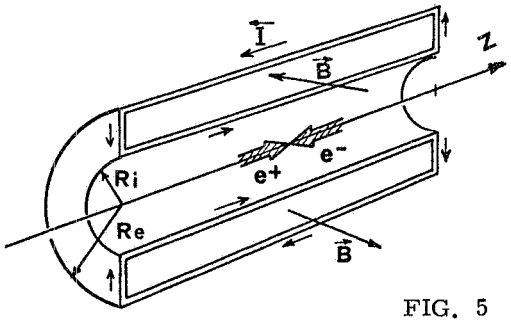

FIG. 5

face as a coil through which the current flows along the two cylindrical surfaces (with the direction of the internal surface opposite to that of the external surface - see aga in Fig. 5) the lines of flux of the field are circles centered on the axis of the beams and in planes perpendicular to them; hence the field is completely contained within the toroidal surface (that is, the coil). Its value is the same at every point on a cylindrical surface coaxial to the beams and is a function only of the radius R according to $B(R) = (R_i/R)\,B(R_i)$, where $R_e \geq R \geq R_i$, with R_e and R_i radii of the cylindrical surfaces external and internal to the torus. For $R < R_i$ and $R > R_e$ the magnetic field is zero (see Fig. 6).

The resulting magnetic field therefore is always perpendicular to every semi plane emerging from the axis of the beams. Thus the direction of exit of all particles produced belongs to one of these semiplanes. The particle is deflected in it, that is it is deflected only in zenith (θ) and not in azimuth (φ) (see Fig. 7). It is then possible to realize a very simple logic for the trigger, accepting simultaneously all the possi ble final states of each reaction (excluding possibly the reactions with all neutral products).

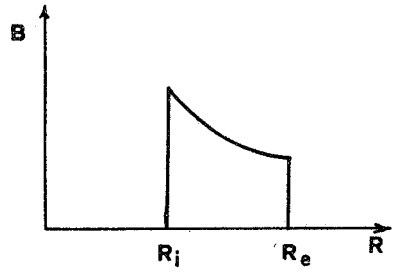

FIG. 6

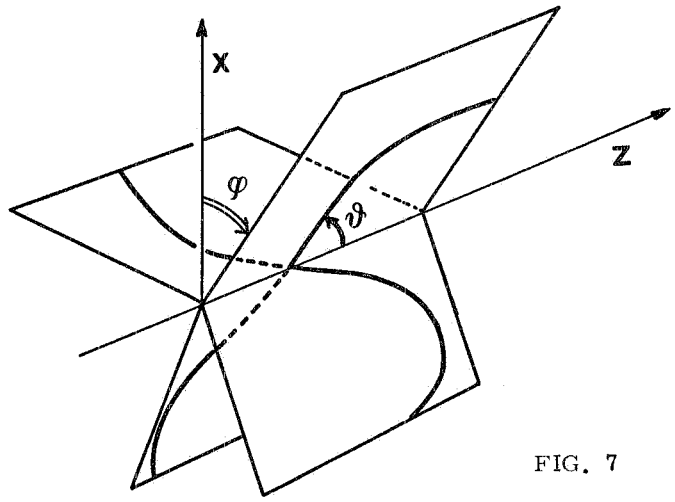

FIG. 7

In the paragraphs which follow a possible solution for Adone with toroidal field produced by a aluminium coil (MAT1) will be discussed, and another possible solution utilizing a coil realized with superconducting wires (MAT2) will be only men tioned. Finally different systems for the detection of trajectory curvature will be con sidered: these systems bring about some simplifications in the above solutions.

3. - EVALUATION OF A "TOROIDAL" MAGNETIC FIELD FOR ADONE PRODUCED BY A ALLUMINIUM COIL (MAT1). -

If it us desired to utilize a very simple coil that fully exploits the capabilities of the power-supply(x) without however reaching in the aluminium currents near the limits of technical possibility, it is necessary that the thickness $s(R_i)$ of the internal cylinder be somewhat high, a few cm for $B(R_i) > 5$ KGauss. Then the principle geo-

(x) - The power-supply which is expected to be used is that acquired for MEA, with the usable power of 1.8 MW and with a current of 5000 A at 400 Volts.

metrical parameters become nearly determined by the scattering (whether coulomb or nuclear) which the particles undergo in traversing this thickness. This scattering in fact imposes two conditions : a) constraining the measurement of the direction of the particle for $R < R_i$ (that is outside the volume enclosed by the coil), fixing the minimum value possible for R_i ($\gtrsim$ 25 cm) ; b) fixing the maximum thickness $s_i = s(R_i)$ acceptable for not losing too many particles, and hence fixing the maximum value obtainable for the field (see Fig. 8). The percentage momentum resolution is roughly

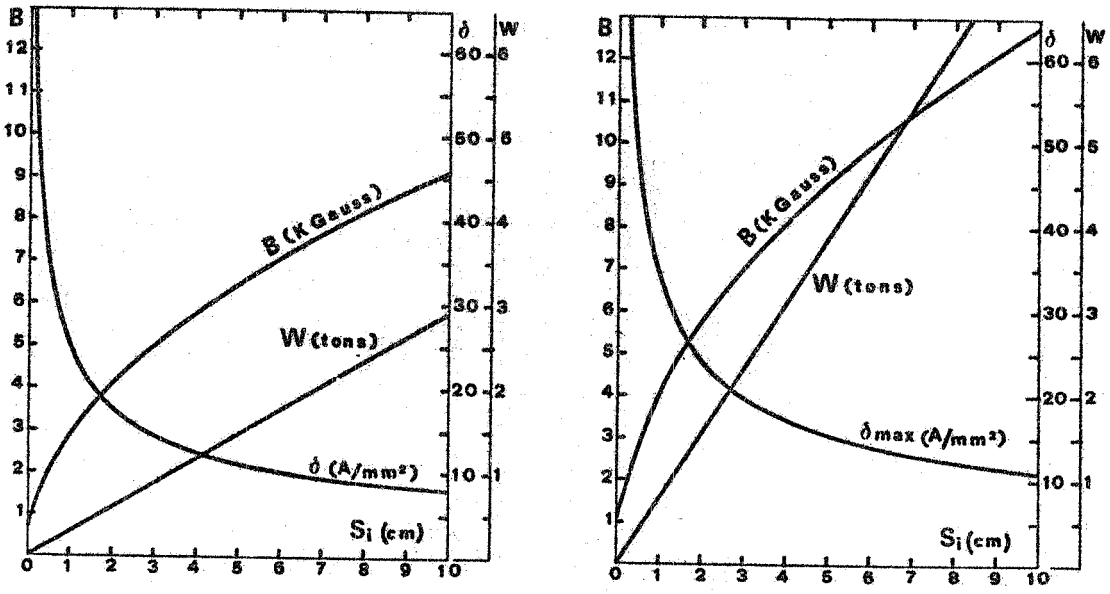

FIG. 8

inversely proportional to $\bar{B}L^{\alpha}$ (where L is the length of the path of the particle in the magnetic field, and $\bar{B}$ is the average magnetic field along L, and $\alpha = 1.5 \div 2.0$) up to $L \sim 100 \div 200$ cm, after which the dependence on L gets less ($\alpha \lesssim 1.5$) for the main error is due to scattering of the particle by material in the measurement apparatus and by the air : for this reason (besides considerations of weight and cost) it is not convenient to make L too long - assuming an average L of $\sim$ 100 cm on a $\Delta\theta = 40^{\circ}$-$150^{\circ}$ we obtain $R_e \sim 80$ cm + R_i.

With R_i and R_e so fixed and with a reasonable use of the space at disposal in a straight section of Adone the resulting geometrical situation is that illustrated in Fig. 9. The corresponding curves for the magnetic field produced, the current density in the coil and its weight as functions of thickness $s(R_i)$ are reported in Fig. 8a). To choose now the value of $B(R_i)$ it is necessary to make a compromise between the thickness $s(R_i)$ acceptable for the trajectory and $\Delta p/p$ desired, keeping the maximum possible power fixed to 1.8 MW (see note of page 4).

Supposing that the sagitta of the trajectory can be measured to ± 0.3 mm one has for $\Delta p/p$ the values reported in Fig. 10 as a function of p and for a few values of $B(R_i)$ and θ. The parameters reported in Table I, a) refer to the geometrical conditions of Fig. 9 with $s(R_i)$ = 30 mm of aluminium ($\sim 1/3\ \lambda_{rad}$ and $\sim 1/10\ \lambda_{coll}$). An enlargement of the conductor in the outer cylinder of the torus can reduce the power dissipated there and indeed increase the magnetic field, $s(R_i)$ being the same. If we choose for the outer cylinder the same thickness as for the inner one we get a

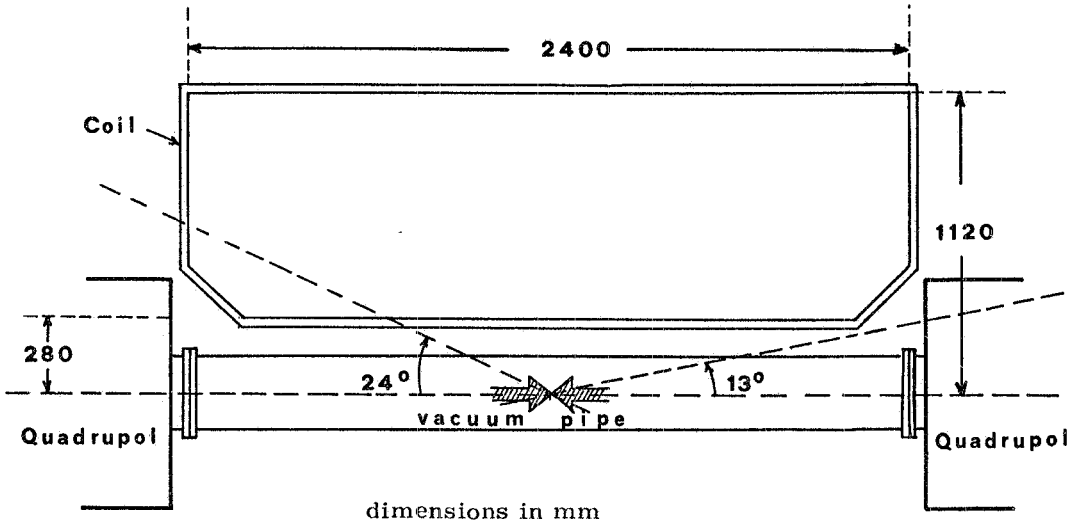

dimensions in mm

FIG. 9

TABLE I - Characteristics of MAT 1 magnet.

		a)	b)
Material of the coil		alluminium	alluminium
Length of the coil	(cm)	240	240
R_i = radius of the inner cylinder	(cm)	28	28
R_e = radius of the outer cylinder	(cm)	112	112
Average thickness of material of the inner cylinder	(mm)	30	30
Average thickness of material of the outer cylinder	(mm)	7.5	30
Current density in the inner cylinder	(A/mm^2)	14.1	19.7
Current density in the outer cylinder	(A/mm^2)	14.1	4.9
Section of the conductor : inner cylinder	(mm^2)	350	350
: outer cylinder	(mm^2)	350	1450
Magnetic field at $R = R_i$	(KGauss)	5	7
Magnetic field at $R = R_e$	(KGauss)	1.25	1.75
Weight of the coil	(tons)	0.87	2.42
Estimate of the price of the coil	$(ML)^{(x)}$	5	10 ÷ 20

(x) - ML = 10^6 Italian Lire $\simeq$ 1700 $ U.S.

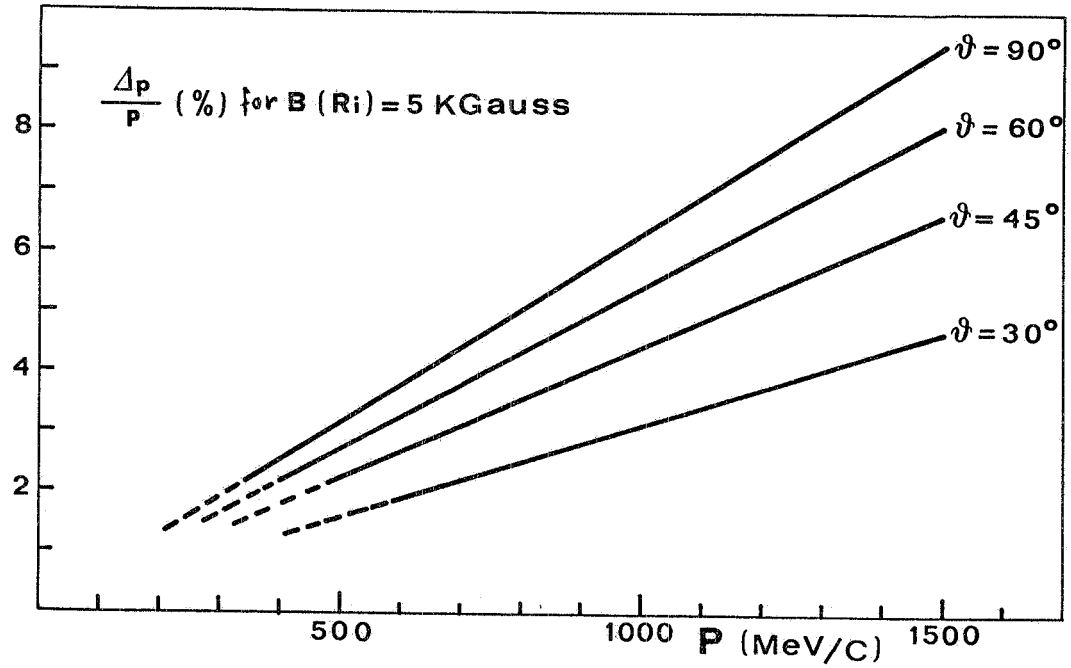
Δp/p (%) for B (Ri) = 5 KGauss
ϑ = 90°
ϑ = 60°
ϑ = 45°
ϑ = 30°
8
6
4
2
500
1000
P (MeV/C)
1500

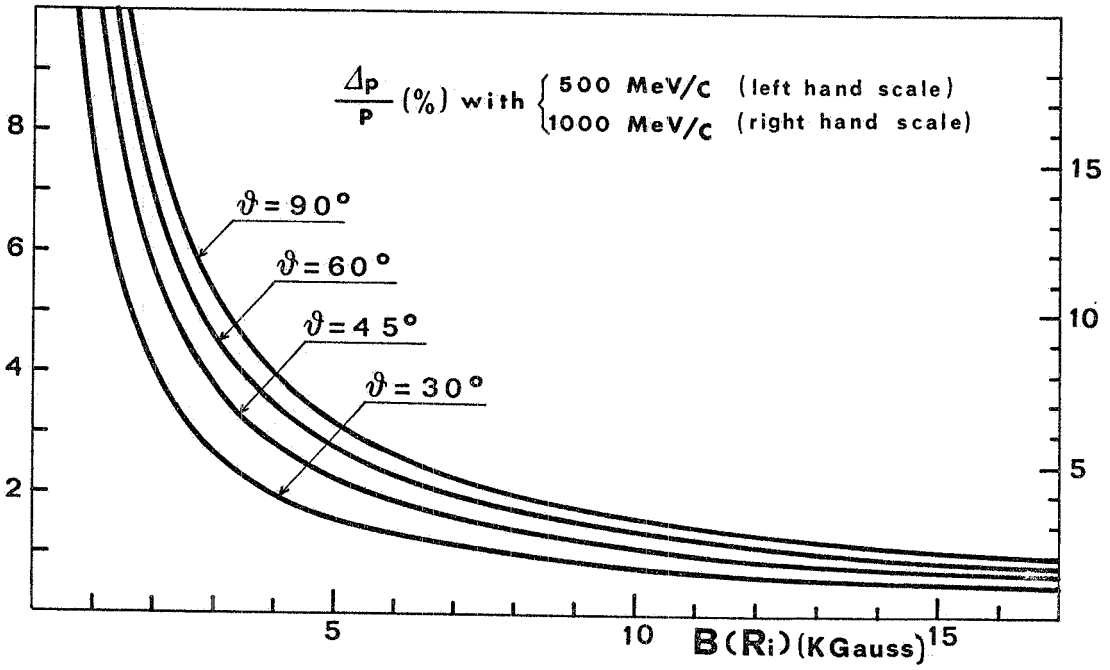
Δp/p (%) with { 500 MeV/c (left hand scale)
1000 MeV/c (right hand scale)
ϑ = 90°
ϑ = 60°
ϑ = 45°
ϑ = 30°
8
6
4
2
15
10
5
5
10
B (Ri) (KGauss)
15

FIG. 10

field a factor ~ 1.4 higher ($B(R_i) = 7$ KGauss ; see Fig. 8b), that shall be payed for by a factor ~ 2 in the weight of material (W = 2.3 tons ; see again Fig. 8b) and in a serious difficulty of construction, since it is a question of winding a conductor with a variable section. For example the parameters concerning this solution are reported in Table I, b).

In Fig. 11 is presented in a longitudinal section the scheme of an experimental apparatus(x), that can possibly be realized by a completely digitized system of coaxial cylindrical wire chambers : a core of 2 or 3 cylinders of proportional wire

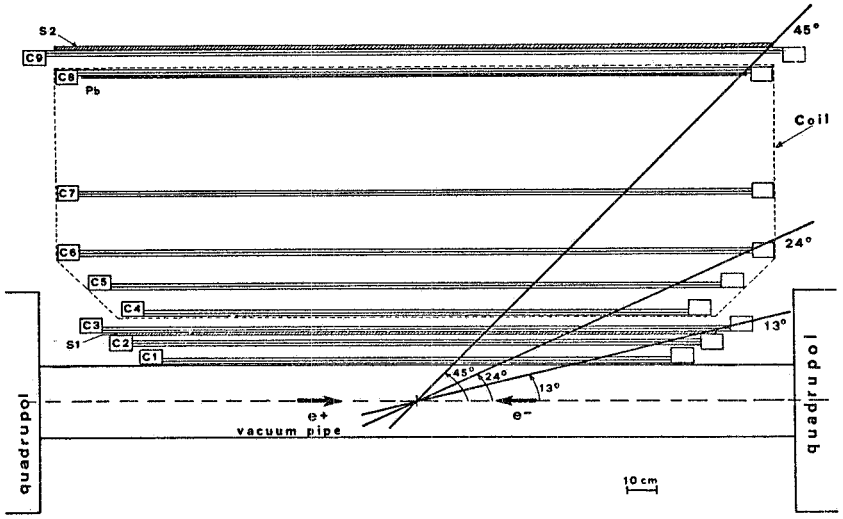

FIG. 11

chambers to measure the direction and to construct the trigger(o) and at least 4 cylinders of magnetostrictive and/or proportional wire chambers for the measurement of the curvature in the magnetic field. For the detection of photons, a solution proposed in (11) can be used joining a radiator of Pb right before the most external chamber and possibly another wire chamber and/or a matrix of counters(+) outside and completely around the coil. For photons with $\theta \lesssim 40^o$ the internal surface of the coil itself furnishes a good radiator ($> 0.6\ \lambda_{rad}$) and the radiative products can be seen by chambers placed within the magnetic field and treated as charged particles. In such a manner photons can be detected up to very low energies and with a good efficiency in a solid angle identical to that used for the measurement of the momentum of the charged particles. An event contaning both charged products and photons can be presented with a projection in the plane (x, y) as a type in Fig. 12.

The scheme of Fig. 11 does not indicate other possible devices (like scintillation or Cerenkov counters or range telescopes) that are always possible to add out-

---

(x) - The coil is only indicated by dotted lines.

(o) - This core can be constructed and used indipendently from the magnet, and it is itself an experimental apparatus nearly complete and usefull whether in experiments for studying multi-hadron production or as central core of other experiments.

(+) - These can be used for the rejection of cosmic rays if it is desired to accept also events with only two collinear particles in the final state.

1 - Vacuum pipe

2 - Region for direction measurement

3 - Region for momentum measurement and for detection of γ-rays at little θ

4 - External region.

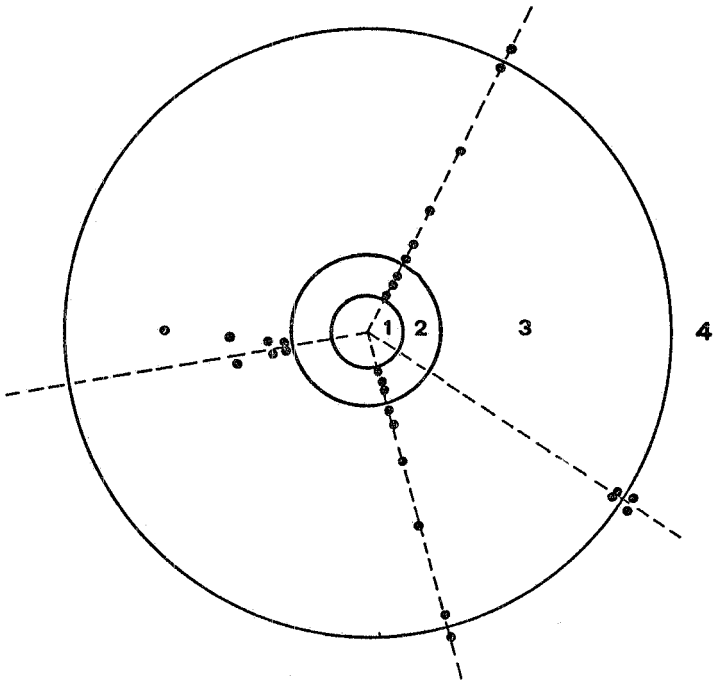

FIG. 12

side, all around or in a portion of solid angle, for recognizing the nature of the particles.

The solid angle available for the measurement of the direction is (for a point source) 97.4 % of the total. With this solid angle the probability of missing one of the particles of an event with 4, 6 or 8 particles produced is about 9.8 %, 14.4 % and 18.6 % respectively (compare Fig. 3 and page 2). The solid angle with which it is possible to measure the momentum with a track length of at least 50 cm is 91.4 % of the total. The variation of the solid angle with the movement of the point source along the axis of the beam is compared in Fig. 13 with that of MEA and MAL.

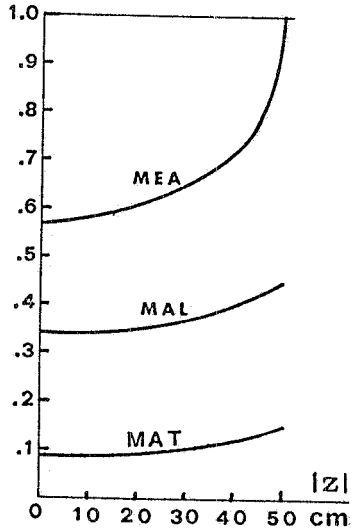

FIG. 13 - Fraction of solid angle not covered by indicated magnets, as a function of the coordinate |z| of the interaction point.

We note, finally, that a solution of the type MAT (either this or any other) avoids completely the problem of the mechanical linking with the machine and of the accesibility of the experimental apparatus.

First of all the external cylinder and the two lateral circular crowns can be realized like an open "fan" (see in Fig. 14 an "artistic view" of the coil); in this manner the accesibility is complete from each side and all around, while the magnetic field is only a little distorted, and only in the region where it is weakest, indeed the measurement of p is not affected. Moreover the coil can be realized in sectors, each

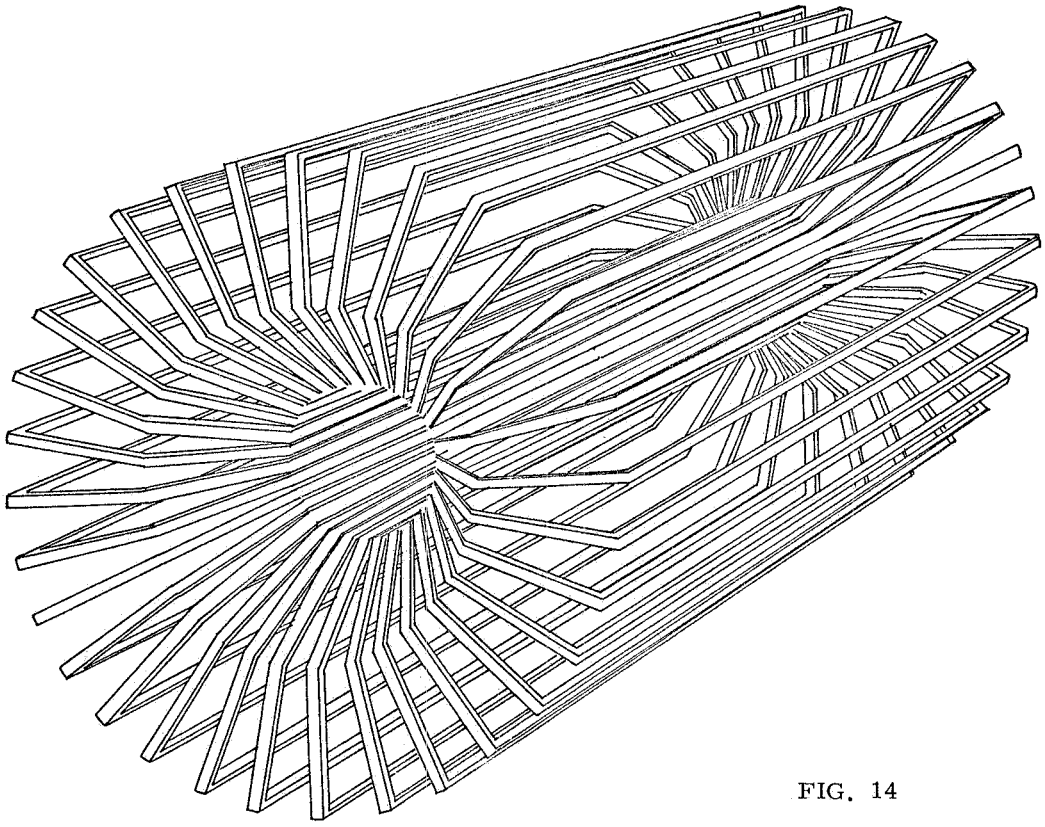

FIG. 14

one complete for its part of the apparatus, almost constituting an experimental apparatus as it stands. These are placed adjacent to eachother and electrically connected for measuring and are set apart from eachother if need be(x). A possible mounting is shown in Fig. 15, a. In case of need some sectors can be removed from the apparatus, without distorting excessively the field within the sectors which remain (see Fig. 15, b). This result is particularly useful if it is desired to use it for performing missing mass of inclusive experiments (see Fig. 15, c), or for detection of the particles with optical apparatus.

(x) - It must be noted that in such an arrangement a portion of solid angle can be lost for obstructions due to frames of chambers and for distortions of magnetic field at the junctions between the sectors of the coil.

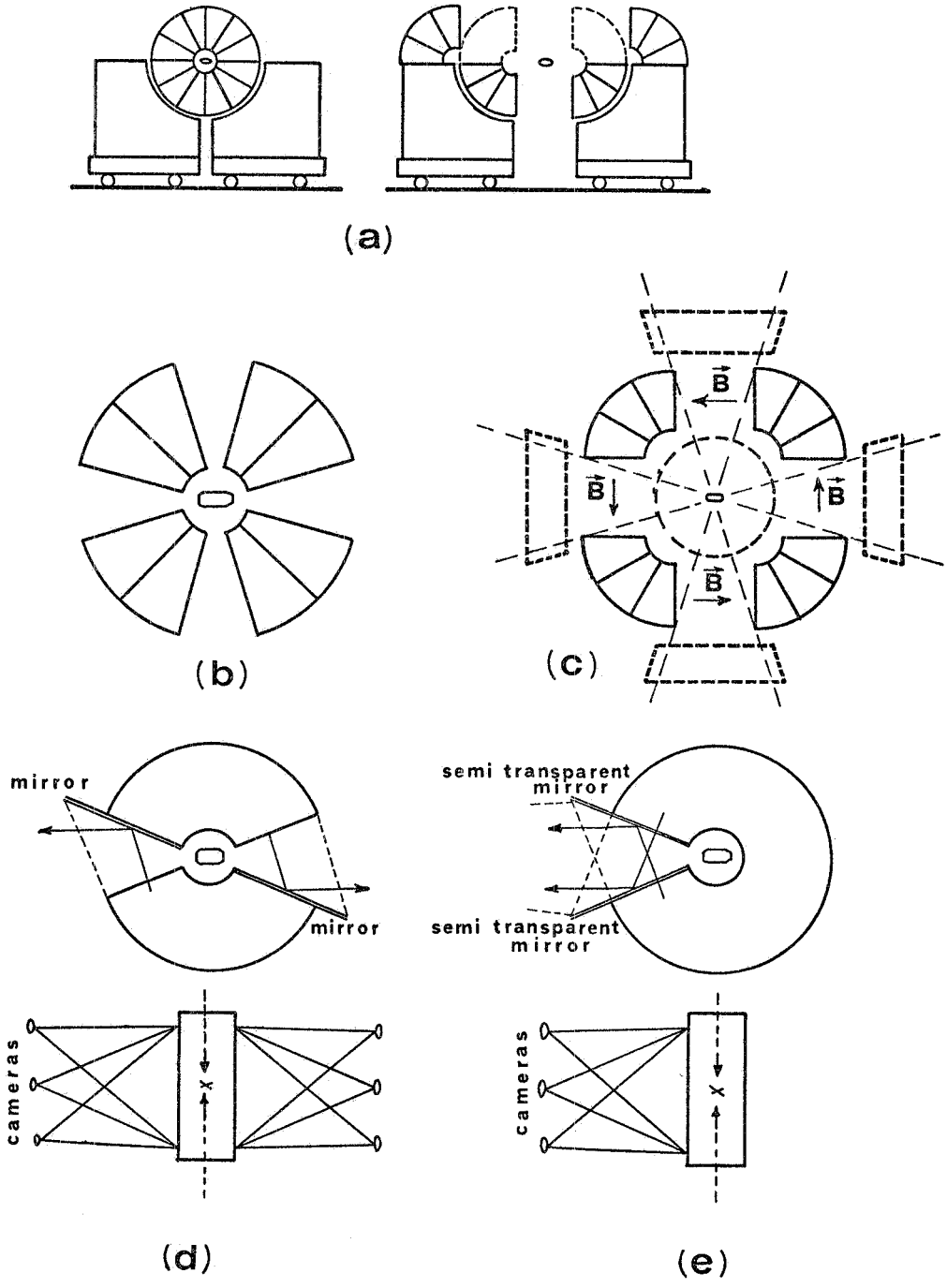
(a)
(b)
(c)
B
B
B
B
(d)
mirror
mirror
cameras
X
(e)
semi transparent mirror
semi transparent mirror
cameras
X

FIG. 15

As examples two schemes of use of an optical apparatus inside a MAT magnet are shown in Figs. 15, d and 15, e : the loss of solid angle are 20% and 10% respectively.

However an optical apparatus can be used inside a MAT magnet without any special mounting of the coil, but simply using its "open fan" structure, as indicated in Fig. 16 ; the loss of solid angle for this case is 9. 8%.

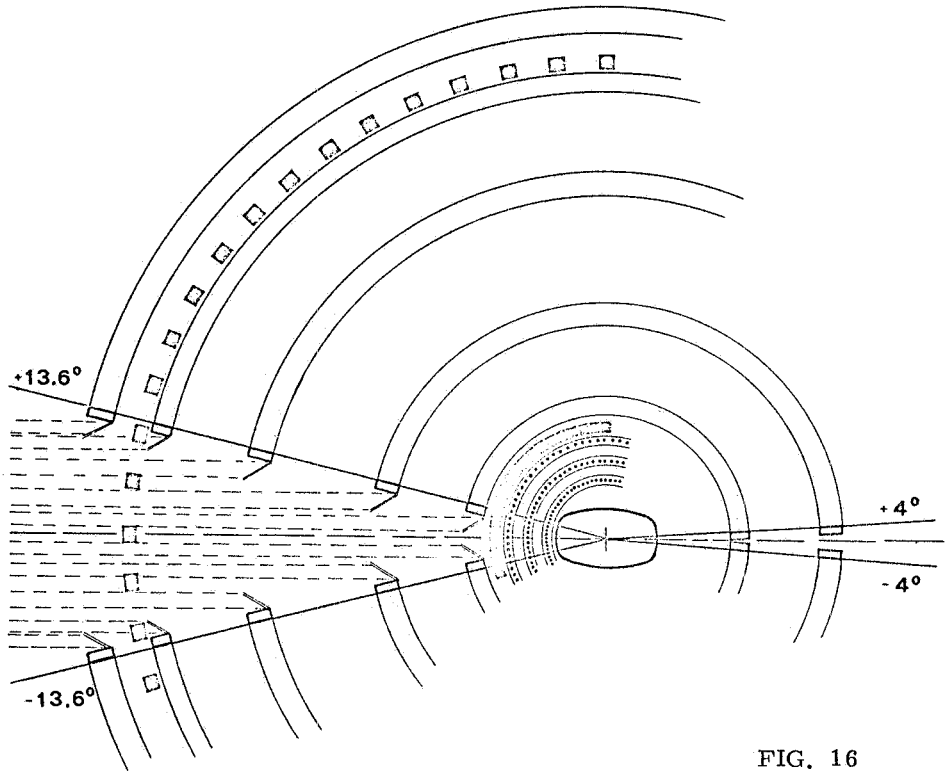

FIG. 16

4. - TOROIDAL MAGNET WITH SUPERCONDUCTING COIL (MAT 2). -

As already has been said above the absence of flux external to the coil and of magnetic linking with the beam renders it possible to think about the use of high values of the field and hence to coils of superconducting wires. For the same $\Delta p/p$ obtainable with the same precision of 0. 3 mm in the "sagitta" of the trajectory would come a very large reduction in the external dimension of the magnet, allowing a maximum radius $R_e \sim$ 60-65 cm provided that we can obtain a field $B(R_i) \simeq$ $\simeq$ 15-20 KGauss. The superconducting wires are immersed in a packet of copper and this is cooled from the outside by liquid helium in $\sim$ 2 mm of steel. A coil so realized can exceed a current density of $\sim$ 150 A/mm^2 provided it does not reach a field too high for which the maximum current density diminishes. In practice, if one accepts a thickness for trajectories of 1 cm of copper ($\sim 1/12\ \lambda_{coll}$ and $\sim 2/3\ \lambda_{rad}$) one obtains $B(R_i)$ = 18. 75 KGauss with a current density of 150 A/mm^2: That means that with the geometry of Fig. 17 one obtains $\Delta p/p$ equivalent to that of

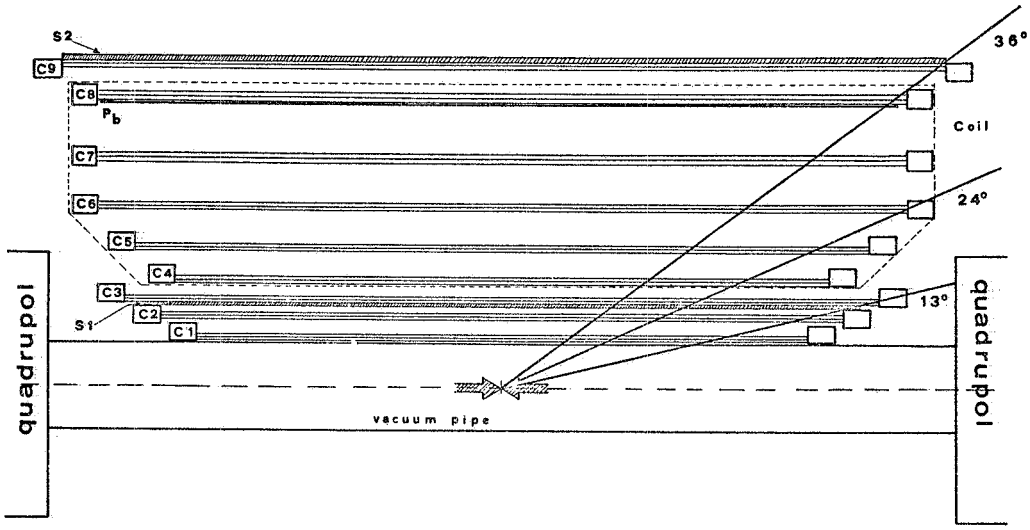

FIG. 17

MAT 1 (see Fig. 10) measuring the sagitta X to ± 0.63 mm. The price of the coil itself is acceptable (~ 25 ML), and can be diminuished substantially by some reduction in the geometry of Fig. 17. The power supply must have the capacity to give high currents ($\sim 10^3$ Ampere) at a few tens of volts, and hence the power supply of MEA becomes wasted for this use. It is indeed convenient to acquire a proper power supply (price $\lesssim$ 5 ML).

The main expenditure will be for the installation for the cooling of the coil with liquid helium of the order of 50 ML or more.

These parameters plus other characteristics of the MAT 2 solution are reported in Table II.

TABLE II - Characteristics of MAT 2 magnet.

Material of the coil		NiTi wires in Cu
Length of the coil	(cm)	240
R_i = radius of the inner cylinder	(cm)	28
R_e = radius of the outer cylinder	(cm)	84
Average thickness of material (Cu) of the inner cyl.	(mm)	10
Average thickness of material (Cu) of the outer cyl.	(mm)	3.3
Thickness of material (Fe) for the circuit of liquid He	(mm)	2
Current density	(A/mm^2)	150
Magnetic field at $R = R_i$	(KGauss)	18.75
Magnetic field at $R = R_e$	(KGauss)	6.25
Estimate of the price of the superconducting wire	(ML)	$\sim$ 25
Estimate of the price of the power supply	(ML)	$\lesssim$ 5
Estimate of the price of the circuit for He	(ML)	$\gtrsim$ 60
Estimate of the price of the dewar for He	(ML)	$\sim$15

Table III reports a comparison between the characteristics of the various magnets proposed for experimentation with Adone.

TABLE III - Comparison between the characteristics of the various magnets proposed for experimentation with Adone.

	MEA	MAL	MAT 1	MAT 2
Solid angle for momentum analysis, $\Delta\Omega_c$	$0.43 \times 4\pi$	$0.66 \times 4\pi$	$0.91 \times 4\pi$	$0.91 \times 4\pi$
Solid angle for detection of photons, $\Delta\Omega_N$	$0.27 \times 4\pi$	$0.71 \times 4\pi$	$0.91 \times 4\pi$ ($\varepsilon \gtrsim 0.4$) $0.71 \times 4\pi$ ($\varepsilon \gtrsim 0.7$)	$0.91 \times 4\pi$ ($\varepsilon \gtrsim 0.4$) $0.80 \times 4\pi$ ($\varepsilon \gtrsim 0.7$)
$\frac{\Delta p}{p}$ for pions at 1 GeV/c (assuming an error of ± 0.3 mm in sagitta)	0.20(o)	0.045	0.063 ($\vartheta = 90^o$) 0.044 ($\vartheta = 45^o$)	0.030 ($\vartheta = 90^o$) 0.021 ($\vartheta = 45^o$)
Energy threshold for trigger (pions at $\vartheta = 90^o$)	110 MeV	65 MeV	< 10 MeV	< 10 MeV
Energy threshold for momentum measurement (pions at $\vartheta = 90^o$)	110 MeV	65 MeV	54 MeV	49 MeV
Material before trigger counters gr/cm^2	37	22	0.6	0.6
λ_{coll}	0.51	0.14	0.024	0.024

5. - DIFFERENT SYSTEMS OF TRAJECTORY CURVATURE DETECTION AND THE CONSEQUENT SIMPLIFICATIONS IN MAT1 AND MAT2 SOLUTIONS. -

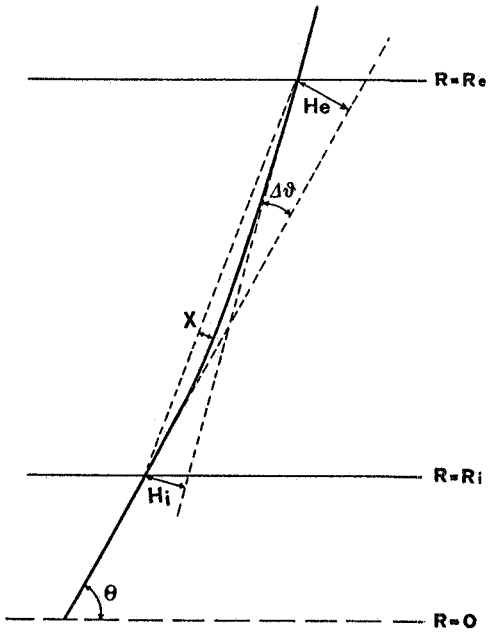

FIG. 18

The schemes of the apparatus for the above mentioned solutions MAT1 and MAT2 (and consequently also the choices for the characteristics of magnets themselves) are the result of considering the momentum measurement through the measurement of the sagitta X of the trajectory.

However, since magnets of MAT type are free from the ingombrance due to iron needed to return the flux we can try a momentum determination through the measurement of the angular deflection ($\Delta\theta$) of the trajectory or of its initial (H_i) or final (H_e) displacement in the magnetic field region (see Fig. 18)(x). The quantities $\Delta\theta$, H_i and H_e are compared in Fig. 19, a and 19, b with the sagitta X in the case of the MAT1 and MAT2 solutions; the explicit computations of these quantities are reported in the Appendix. The percentage error on these quantities due to coulomb scatter-

(o) - Assuming an error of ± 0.15 mm on each point measured on the track.
(x) - For initial (final) displacement we mean the distance of the entrance (exit) point of the particle in (from) the magnetic field from the tangent to its exit (entrance) point.

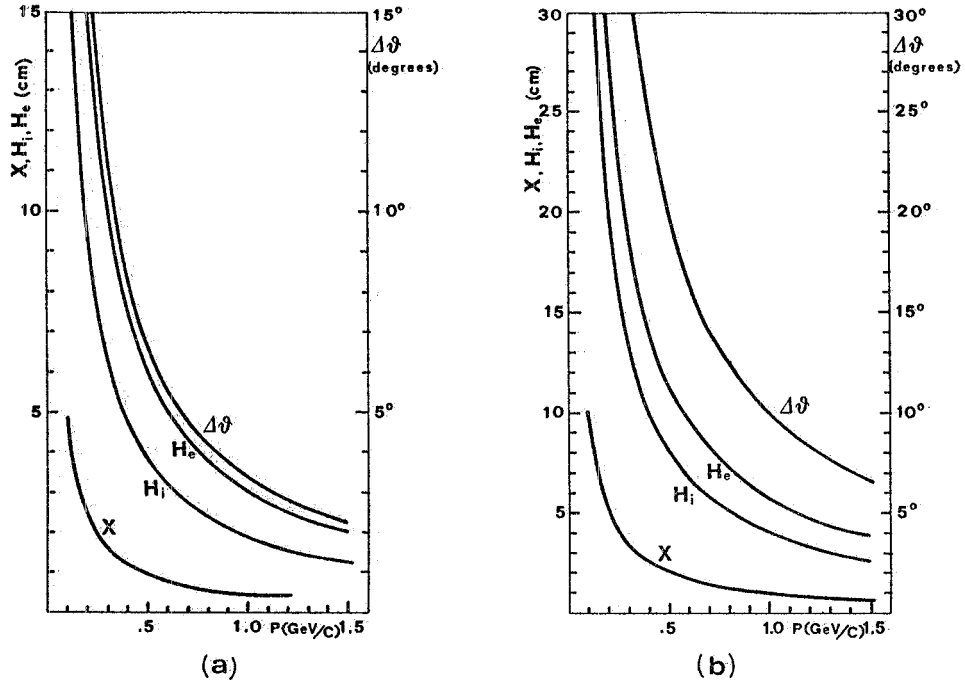
X, Hi, He (cm)
Δϑ (degrees)
Δϑ
He
Hi
X
P(GeV/c)
(a)
(b)

FIG. 19

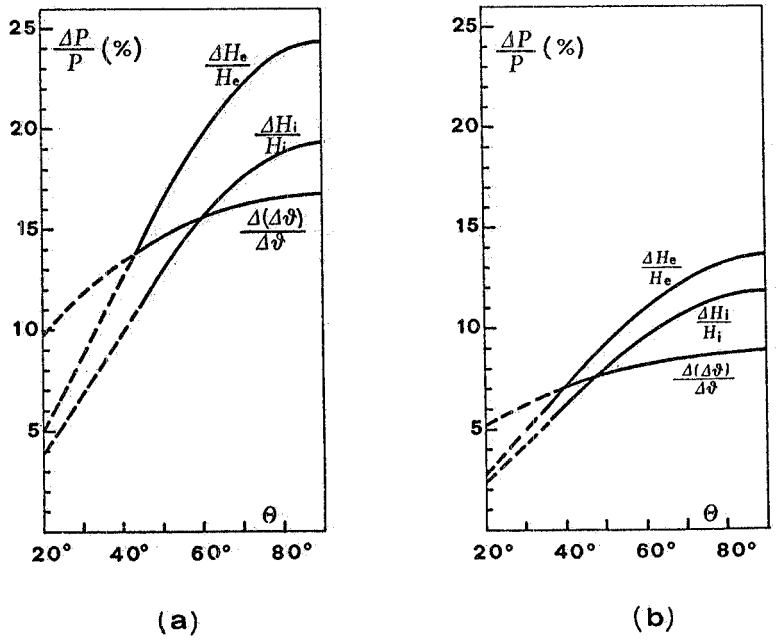
ΔP/P (%)
ΔHe/He
ΔHi/Hi
Δ(Δϑ)/Δϑ
Θ
(a)
(b)

FIG. 20

ing of the particle in the coil is approximatively independent of the momentum; it is reported in Figs. 20, a and 20, b as a function of the angle θ of emission of the particle.

In the following we will examine the simplifications that come to the apparati for the MAT1 and MAT2 magnets using some of these quantities for the momentum measurement.

Case (a) : MAT1 - It is clear that in the case of MAT1 a measurement of $\Delta\theta$ or H_i must be done with chambers outside and around the magnet, excessively large in dimensions if we wish to cover a large solid angle, considering also that the requested angular resolution must be good ($\sim \pm 0.5^o$) (see Fig. 21)(x). On the contrary it is sufficiently easy to measure H_e (see Fig. 22)(o), but the Coulomb scattering in coil material creates a too large an error ($\lesssim \pm 19\%$) in the momentum.
However we can obtain a fairly good measurement of H_i using the fact that the intensity of magnetic field decreases by a factor of 4 from $R = R_i$ to $R = R_e = 4R_i$; in fact the variation $\delta\theta$ of the angle θ_t of the tangent to the trajectory near the exit of the particle from the magnetic field is much smaller than the total deflection $\Delta\theta$ and furthermore it is possible to correct $\Delta\theta$ "a posteriori", when the momentum is roughly determined. For example, using for measurement of the angle θ_t two points at $R = 3R_i = R_c$ and $R = 4R_i = R_e$, we have in H_i a systematic (and correctable) error of -26% (i.e., $H_i = 0.74\, H_i$) for any momentum (see Fig. 23). If the position at $R = R_i$ and the angle θ_t can be determined respectively to ± 1 mm and $\pm 0.2^o$ (i.e., $\sim \pm 0.7$ mm in each point), the precision in momentum is that reported in Fig. 24 as a function of momentum and for some value of θ_i. Only the multiple scattering at $R = R_c$ contributes to the error and can be neglected if the material at $R = R_c$ is less than $\sim 0.05\ \lambda_{rad}$.

Case (b) : MAT2 - In the solution MAT2 the limiting precision permitted by multiple scattering is sufficient if we measure $\Delta\theta$, and it is still useful if we measure either H_i or H_e. However practicaly a measurement of $\Delta\theta$ or H_i makes the dimensions for the external chambers problematic (but see again Fig. 21 and note (x) of this page), and indeed, from this point of view, a measurement of H_e is certainly preferible although the multiple scattering makes the resulting momentum measurement less precise ($\pm 11.8\%$ at any momentum and at $\theta = 90^o$; see Fig. 20, b).
Also in this case we have recourse to a measurement of H_i as realized in the case of MAT1. Using for the measurement of θ_t two points at $R = 2.5\, R_i = R_c$ and $R = 3R_i = R_e$ we have $H_i^{meas} = 0.85\, H_i$, and we get the same precision as in the case of MAT1 (see again Fig. 24) provided that the position at $R = R_i$ can be determined to ± 5 mm and the angle θ_t to $\pm 0.57^o$ (± 1 mm at each point), and the thickness of the material interposed in trajectory inside the magnetic field is less than $0.4\ \lambda_{rad}$.

(x) - However we can have recourse to a measurements of the angle θ_t to the exit tangent to the trajectory through optical chambers (as indicated in Fig. 21) profiting from free space around the coil. In this case the trigger is constructed by the proportional wire chambers around the vacuum pipe, and the trigger to the optical chambers is given only for events that require the measurement of some momenta for a complete reconstruction.

(o) - It is sufficient to measure θ to $\sim \pm 0.8^o$ in the directional wire chambers inside the internal cylindrical surface of the torus, and the outgoing point of trajectory from the magnetic field to $\sim \pm 5$ mm.

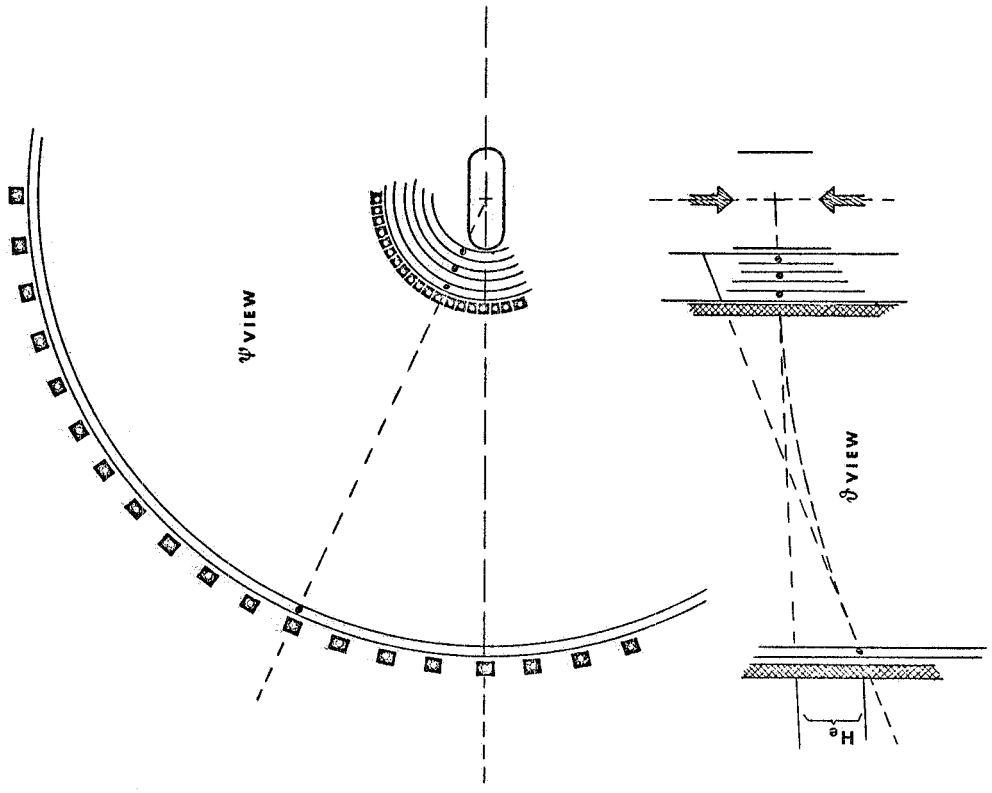

FIG. 22

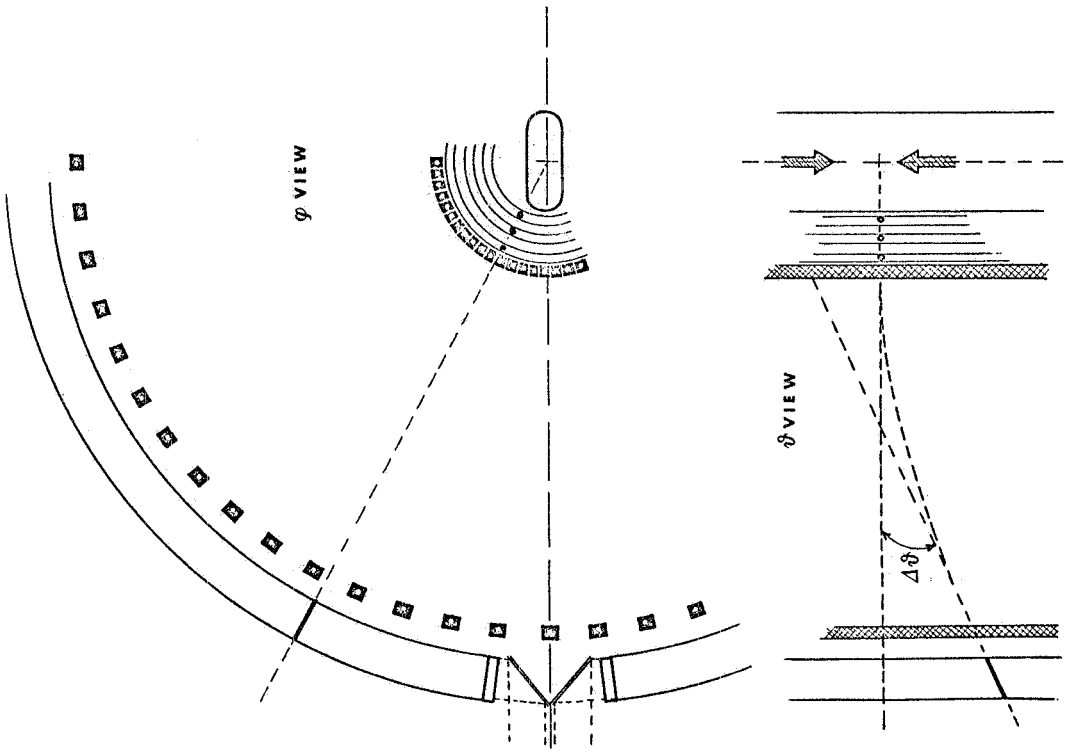

FIG. 21

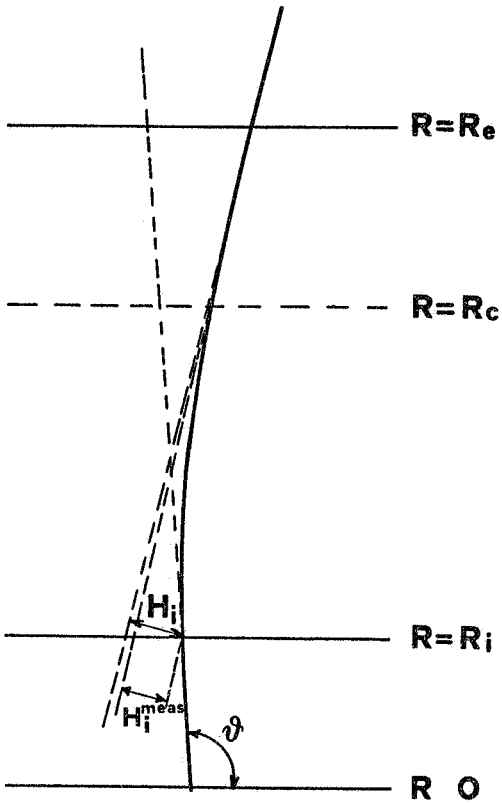

FIG. 23

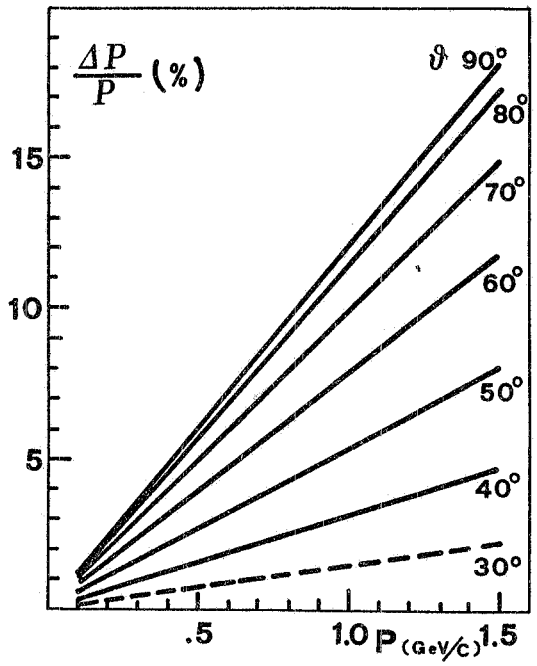

FIG. 24

Finally, must be stressed that the aim of this work is a preliminary study of the experimental possibilities on Adone of a MAT type magnet. Technical evaluations and estimates of prices will be successively examined in an eventual detailed project.

APPENDIX. -

The equation for the radius of curvature ρ of a particle of charge q and momentum $\vec{p}$ in a magnetic field $\vec{B}$ perpendicular to $\vec{p}$, is

$$\frac{1}{\rho} = \frac{q}{p} B . \tag{A. 1}$$

If $\vec{p}$ remains always perpendicular to $\vec{B}$ (plane trajectory) the differential equation of the trajectory in ortogonal cartesian coordinates (x, y, z) is given by[12]:

$$\frac{d^2z}{dx^2} + \frac{q}{p} B_y \left[1 + \left(\frac{dz}{dx}\right)^2\right]^{3/2} = 0 . \tag{A. 2}$$

When $B_y(x, z)$ is known this equation can be resolved (possibly with numerical methods) furnishing the "ray tracing" corresponding to given initial conditions z(0) and $\frac{d^2z}{dx}(0)$.

In the case of a MAT magnet we can assume a reference system where x axis is the direction of emission of the particle ($x = R/\text{sen}\,\theta$), y axis is parallel to the magnetic field $B_y = B_y(R)$, and z axis is perpendicular to the plane (x, y) (see Fig. 25). The motion of the particle is in the plane (z, x).

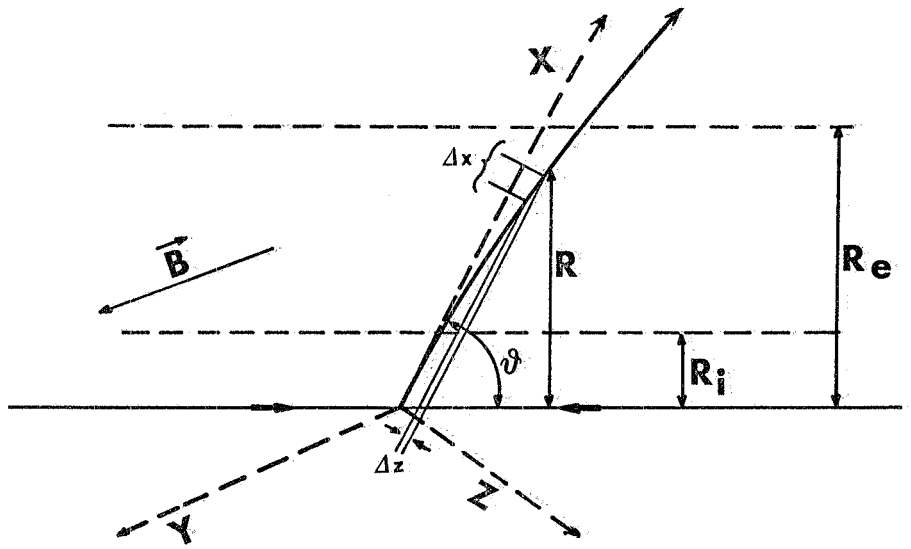

FIG. 25

For a particle with sufficiently high momentum $(dz/dx)^2 \ll 1$ (see Fig. 25); hence we can expand the second addend of equ. (A. 2) in a serie of $(dz/dx)^2$, stopping up to the linear term:

$$\frac{d^2z}{dx^2} + \frac{qB_y(R)}{p}\left[1 + \frac{3}{2}\left(\frac{dz}{dx}\right)^2\right] = 0$$

and since $x = R/\text{sen}\,\theta$

$$\frac{d^2z}{dR^2} + \frac{qB_y(R)}{p\,\text{sen}^2\theta}\left[1 + \frac{3\,\text{sen}^2\theta}{2}\left(\frac{dz}{dR}\right)^2\right] = 0 . \tag{A. 3}$$

If $dz/dR \lesssim 0.2 - 0.3$ (what means $p \gtrsim 100$ MeV/c for MAT1 and MAT2) we can simplify further this equation, obtaining directly the second derivative of the trajectory:

$$\frac{d^2z}{dR^2} = - \frac{q\, B_y(R)}{p\, \mathrm{sen}^2\theta} \quad .$$

In a MAT magnet $B_y(R) = B(R_i)\,\frac{R_i}{R}$ and we get:

$$\frac{d^2z}{dR^2} = - \frac{q\, B(R_i)\, R_i}{p\, \mathrm{sen}^2\theta}\,\frac{1}{R} \quad . \tag{A. 4}$$

Integrating this equation from R_i to a arbitrary R we obtain:

$$\frac{dz}{dR} = - \frac{q\, B(R_i)\, R_i}{p\, \mathrm{sen}^2\theta}\, \lg\, \frac{R}{R_i} \quad . \tag{A. 5}$$

The "displacement" of the trajectory (as defined in Fig. 18 and in note of page 14) at $R = R_e = MR_i$ (final displacement) is obtained from integration of eq. (A. 5) from R_i to R_e:

$$H_e = - \frac{q\, B(R_i)\, R_i^2}{p\, \mathrm{sen}^2\theta}\, (M \log M - M + 1) \,. \tag{A. 6}$$

The "displacement" of the trajectory at $R = R_c = NR_i$ from its tangent at $R = R_e = MR_i$ is obtained from integration of eq. (A. 5) from R_e to R_c:

$$H_i' = - \frac{q\, B(R_i)\, R_i^2}{p\, \mathrm{sen}^2\theta}\, (M - N - N \log \frac{M}{N}) \,. \tag{A. 7}$$

If $R_c = R_i$ (N=1) we get

$$H_i = - \frac{q\, B(R_i)\, R_i^2}{p\, \mathrm{sen}^2\theta}\, (M - 1 - \log M) \,. \tag{A. 8}$$

The angular deflection $\Delta\theta$ comes directly from integration of $d\theta = dR/\rho$, using for the radius of curvature ρ the equation (A. 1)

$$\Delta\theta = \frac{q}{p} \int B\, ds \,.$$

In the case of a MAT magnet, with the same reference system and the same approximations introduced for dealing eq. (A. 2), is $s = x = R/\mathrm{sen}\,\theta$, and we get:

$$\Delta\theta = \frac{qB(R_i)R_i}{p\,\mathrm{sen}\,\theta} \int_{R_a}^{R_b} \frac{dR}{R} = \frac{qB(R_i)R_i}{p\,\mathrm{sen}\,\theta} \log \frac{R_b}{R_a} = \frac{qB(R_i)R_i}{p\,\mathrm{sen}\,\theta} \log \frac{M}{N} \tag{A. 9}$$

(with $R_a = NR_i$ and $R_b = R_e = MR_i$), which reduces to:

(A. 10) $$\Delta\theta = \frac{q\,B(R_i)\,R_i}{p\,\mathrm{sen}^2\,\theta}\,\log M$$

for $R_a = R_i$ (N=1).

ACKNOWLEDGEMENTS. -

I would like acknowledge G. Pasotti, N. Sacchetti, and M. Spadoni of the Magnet group for helpful discussions and for essential information for the calculations of this work, and K. Ekstrand, guest in Frascati, who helped me with a critical revision of the text.

REFERENCES. -

(1) - M. Grilli, F. Soso, P. Spillantini, M. Nigro, E. Schiavuta e V. Valente, Misura delle annichilazioni in più di due corpi mediante l'uso di un campo magnetico assiale, Presented at the 'Congress for Experiments in Adone', Frascati (1966).

(2) - G. K. O'Neill, A magnetic detector for Adone, Frascati report LNF-66/18 (1966); Presented at the 'Congress for Experiments in Adone', Frascati (1966).

(3) - G. K. O'Neill, Momentum-analysing detector design for 1.5 GeV/c, Presented at the 'Intern. Symp. on Electron and Positron Storage Rings', Saclay (1966).

(4) - M. Bernardini, A. Buhler, P. Dalpiaz, M. N. Focacci, G. Furtunato, T. Massam, Th. Muller, G. Petrucci, F. Saporetti and A. Zichichi, Experimental investigations proposed for Adone, Presented at the 'Congress for Experiments in Adone', Frascati (1966).

(5) - L. S. Osborne, Design of a magnetic analysis system for storage ring experiments (It concerns the magnets of CEA), Presented at the 'Intern. Symp. on Electron and Positron Storage Rings', Saclay (1966).

(6) - A. M. Boyarski, H. Brechna, F. Bulos, R. Diebold and B. Richter, Magnetic detector for a 3 GeV e^+e^- storage rings (It concerns the magnets of the 3 GeV e^+ e^- storage rings of Stanford), Presented at the 'Intern. Symp. on Electron and Positron Storage Rings', Saclay (1966).

(7) - U. Amaldi Jr., G. K. O'Neill, G. Petrucci, G. Sacerdoti e E. Schiavuta, Relazione del gruppo di studio per la sperimentazione con campo magnetico presso Adone, Frascati report LNF-67/3 (1967).

(8) - C. Guaraldo e P. Spillantini, Progetto di misura del contributo dello stato intermedio in 2γ al processo $e^+e^- \rightarrow \pi^+\pi^-$ (Con campo magnetico e camere a scintilla ottiche), Frascati internal report LNF-67/48 (Int.) (1967).

(9) - G. P. Murtas, G. Sacerdoti, M. Nigro, R. Santangelo, E. Schiavuta, D. Scannicchio, D. Grossman, G. K. O'Neill e G. Matthiae, Progetto di un dispositivo sperimentale per l'analisi magnetica dei prodotti di reazione di Adone, Frascati internal report LNF-68/7(Int.) (1968).

(10) - W. Ash, D. Grossman, G. Matthiae, G. P. Murtas, M. Nigro, G. K. O'Neill, G. Sacerdoti, R. Santangelo, D. Scannicchio and E. Schiavuta, A magnetic analyzer to be used for Adone colliding beam experiments, Frascati report LNF-69/2 (1969).

(11) - K. Steffen, Plans for storage ring and detection apparatus at DESY, Report DESY-70/24 (1970).

(12) - G. Sanna, L'ottica degli spettrometri magnetici nella approssimazione del primo e secondo ordine. Parte I: le equazioni differenziali delle traiettorie in forma esatta, Frascati report LNF-71/81 (1971).

(13) - B. Bartoli, D. Bisello, A. Cattoni, D. Cheng, C. Costa, F. Felicetti, P. Monacelli, A. Mulachiè, M. Nigro, H. Ogren, I. Peruzzi, L. Pescara, M. Piccolo, F. Ronga, R. Santangelo, V. Silvestrini e F. Vanoli, Studio di un dispositivo magnetico con campo longitudinale per la sperimentazione con Adone, Frascati report LNF-71/90 (1971).